

DETECTION OF ROCK SLOPE FAILURE PRECURSORS USING A TERRESTRIAL LASER SCANNER



*Challenges from North to South
Des défis du Nord au Sud*

Ryan Kromer, Jean Hutchinson
Queen's University, Kingston, Canada
Matt Lato, Dave Gauthier
BGC Engineering, Ottawa, Canada
Tom Edwards
CN Rail, Edmonton, Canada

ABSTRACT

Here we address the prediction of rockfall, which represents one of the highest risks to transportation corridors in mountainous terrain. In this study, we monitored a slope along the CN Rail line in the Fraser River Valley, BC using terrestrial laser scanning (TLS) to: identify rockfall source areas based on precursor deformation, track the deforming areas in 3D, project their potential volumes and provide early warning to the railway prior to rockfall. We identified three areas of deformation, between December 2013 and June 2014, the largest having a potential failure volume of 4800 m³. Three-dimensional tracking of this block allowed us to identify the failure kinematics prior to failure of the largest block, a wedge type failure plunging at 14° with a vector deformation magnitude of 0.1 m. In September of 2014, we gave warning to the railway of the potential rockfall volume and of the kinematics for the largest identified area. We continued to monitor the deforming areas of the slope until all three rockfalls occurred, in December 2014 after a large rainfall event. We collected oblique helicopter photos for photogrammetric analysis three days post failure and calculated a depletion area volume for the largest block of 4200 m³ and volumes of 210 and 220 m³ for the smaller two deforming areas. This ability to detect, locate and quantify and understand 3D kinematics prior to rockfall has resulted in an improved ability to prioritize mitigation efforts, reduce risk, and better understand slope failure mechanisms.

RÉSUMÉ

Nous abordons ici la prédiction des éboulements, ce qui constitue l'un des risques les plus importants affectant les infrastructures de transport situées en terrain montagneux. Dans cette étude, nous avons utilisé le LiDAR terrestre afin de surveiller une pente rocheuse située le long d'un tronçon d'une voie de chemin de fer du CN, dans la vallée Fraser, en Colombie-Britannique. Les objectifs de cette étude sont d'identifier les zones d'éboulement par les déformations avant-coureurs, de suivre les zones de déformation en 3D, de calculer leurs volumes potentiels, ainsi que de fournir un système d'avertissement préventif. Nous avons identifié trois zones de déformation entre Décembre 2013 et Juin 2014, la plus grande ayant un volume estimé de 4800 m³. Le suivi 3D de cette zone de déformation nous a permis d'identifier les mouvements précurseurs à la rupture. Le mécanisme de rupture de ce dernier a été identifié comme un glissement plongeant à 14° et avec un déplacement de 0.1 m le long de la ligne d'intersection des deux plans. En Septembre 2014, une alerte a été transmise au CN quant à la potentielle rupture de ce bloc. La surveillance des zones instables a été conduite jusqu'à ce que la rupture des trois secteurs instables se soit produite, à la suite d'un épisode pluvieux important en Décembre 2014. Une analyse par photogrammétrie a été effectuée à l'aide de photos prises par hélicoptère trois jours après l'évènement. Cela a permis de calculer un volume éboulé de 4200 m³ pour le plus grand des blocs et des volumes de 210 et 220 m³ pour les deux autres zones d'éboulement. Cette capacité à détecter, localiser et quantifier les mouvements en 3D avant la rupture a résulté en une meilleure gestion de la priorisation des efforts de réduction des impacts, en une réduction des risques, ainsi qu'en une amélioration de la compréhension des mécanismes précurseurs à la rupture en général.

1 INTRODUCTION

Communities and infrastructure in mountainous areas are often vulnerable to various geological hazards, including rockfalls. These types of hazards tend to occur suddenly and their spatial location and time of failure is often unknown a priori and as a result, they represent one of the highest risks to transportation corridors. The Railway Ground Hazard Research Program, a Canadian

collaborative effort between industry, government and universities, aims to better understand the mechanisms that lead to these hazards and to develop tools and technologies to identify and manage them. As part of this research program, we have been monitoring a selection of hazardous slopes across the Canadian rail network, using Terrestrial Laser Scanning (TLS), Terrestrial Photogrammetry, Oblique-Aerial Photogrammetry (OAP), and Aerial Laser Scanning (ALS) (Lato et al., 2011; 2014).

The main advantages of these approaches for monitoring and characterizing ground hazards are:

1. The avoidance of direct exposure of personnel to rock slope hazards.
2. The efficiency and consistency of data collection, and the characterization and monitoring of a slope (e.g. Oppikofer et al., 2008; Sturzenegger and Stead, 2009).
3. The ability to monitor inaccessible areas or areas not otherwise visible from rail level.
4. The capability to interpret small scale changes of the entire slope surface in three dimensions (3D) (e.g. Abellán et al., 2011; Lim et al., 2005; Rosser et al., 2005).
5. The relative affordability compared to other slope scale rockfall monitoring approaches.

A main purpose of this on-going work, addressed in this study, is to better detect precursors to discrete rock slope failure, to quantify potential failure volumes and to assess kinematic prior to failure, so that we can provide early warning, better assess risk and better understand failure mechanisms and triggering factors. This will ultimately improve safety of people and property exposed to many types of slope hazards, particularly rockfall and related landslide types.

Advances in the analysis of remotely sensed 3-Dimensional (3D) point clouds collected in series, permits the detection of precursors prior to rock detachment, which can allow for the identification of potential rockfall source zones (Abellán et al., 2010; Royán et al., 2013). Precursors consist of deformation, smaller volume rock detachments and opening of tension cracks and often progress both in space and time (Rosser et al., 2007; Stock et al., 2012). Precursors are a result of internal failure processes such as fracture propagation and/or sliding along pre-existing fractures within a rockmass (Eberhardt et al., 2004; Petley, 2004). This process often occurs progressively (Stock et al., 2012), which can allow for the prediction of rockfall location and time.

To date, the accurate identification of source zone locations, potential failure volumes and pre/failure kinematics has yet to be realized in a complex slope environment in an operating rail setting. In this study, we used terrestrial LiDAR data at a high activity site to

provide early warning of three discrete rockfall events based on the identification of precursors at a high rockfall activity site along CN Rail line in Southwestern British Columbia. T

1.1 Study Site Description

T

The current study site is located along the CN Rail line (Figure 1), approximately 150 km northeast of Vancouver in the Fraser River valley. The railway line traverses a steep slope composed of a Cretaceous-aged thick succession of shallow water deltaic sedimentary rocks (MacLaurin et al., 2011). Two local scale faults cross cut the rock slope and four main joints sets are described in Sturzenegger et al. (2014) (J1/J4 strike/dip: 349° /88°, 030° /85°, 162° /44° and 301° /84°). In November 2012, a 53 000 m³ rockslide and debris slide occurred at this location, resulting in the collapse of a 21 m long rockfall protection structure and a four-day railway closure (Sturzenegger et al., 2014). Construction of a redesigned structure started in 2013 and was completed in summer of 2014.

1.2 Data Collection and Timeline of Events

We obtained ALS scans in December 2012 and April 2014, and collected several TLS scans from a terrace on the opposite (west) side of the Fraser River valley beginning in December 2013. After eight months of monitoring, we identified three areas of discrete rock block deformation. On 9 September 2014, we gave warning to CN of the largest identified rockfall source area. A qualitative risk assessment was conducted by CN and it was determined that the new rockfall protection structure would provide sufficient protection to the railway. In the months preceding failure we continued to monitor slope deformation using TLS.

On 3 December 2014, a CN engineer noted an accumulation of approximately 20-30 m³ in a draped steel mesh fence located above the rockfall protection structure. On 11 December 2014, following three days of rainfall totaling 41 mm (Environment Canada, 2014), a CN maintenance employee detected a larger accumulation of debris behind the rockfall protection structure.

We were able to assess the rockfall source zones and rockfall run out within three days of the observed accumulation using a detailed 3D photogrammetric slope model generated from a set of oblique helicopter photos (OHP) on 14 December 2014. Due to a scanner malfunction, TLS data collection within a week post failure was not usable.

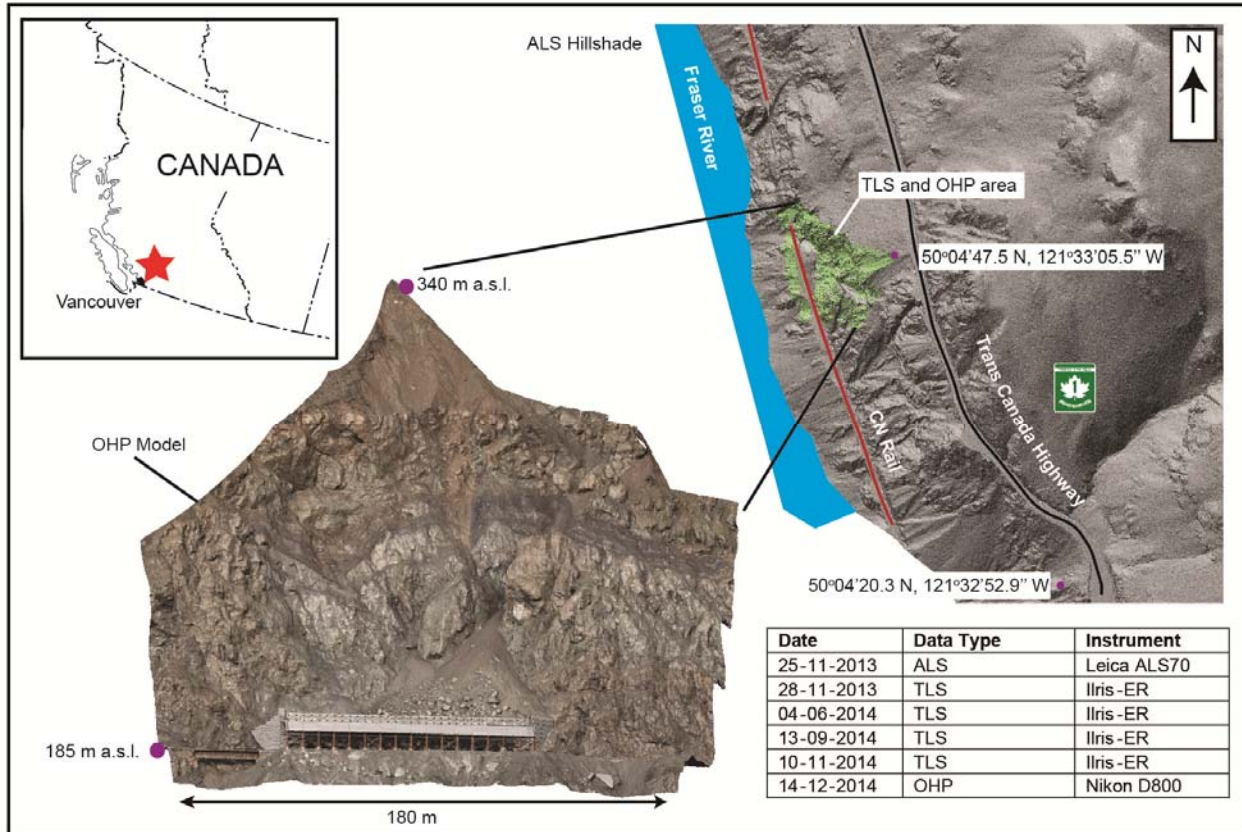


Figure 1: Location of study site and data sets collected. Oblique view of ALS data set (top right), Oblique Helicopter Photos (OHP) and data collection dates (bottom right).

2 MATERIAL AND METHODS

Terrestrial Laser Scanning data were collected, using an Optech Ilris 3D-ER scanner, in four separate data collection campaigns as outlined in Figure 1. This scanner has a range of 1800 m at 80% surface reflectivity and a manufacturer-specified range and angular accuracy at 100 m per point of 7 mm and 8 mm, respectively (Optech, 2014). The area of the slope we monitored with TLS, shown in Figure 1, ranges from 185 to 340 m a.s.l. and spans a 200 m length of railway track. TLS data were collected from two survey stations located on the opposite side of the river valley, providing overlapping coverage of the area of interest, with a minimum and maximum range to slope of 350 and 550 m respectively, resulting in mean point spacing ranging from 0.05 to 0.08 m.

Data alignments were performed in the IMAAlign module of PolyWorks V14 (InnovMetric, 2014) for scans taken on the same date from different survey locations, and between scan dates. The reference TLS scan (28 November 2013) was aligned to the ALS data set and each subsequent TLS scan was aligned to the reference TLS scan using a three-step methodology: (i) manual identification of common points, (ii) implementation of a surface to surface iterative closest

point (ICP) best fit algorithm, and (iii) identification of areas of slope change followed by a reapplication of the best fit algorithm with the identified areas omitted. We ignored all points affected by the construction of the rockfall protection structure in the spring and summer of 2014 from all alignment processes. Interscan alignment error (1 St. Dev) between TLS scans varied from 0.011 and 0.018 m. The 95% confidence interval (0.022 to 0.036 m) represents the single point limit of detection of change for this slope.

To analyze change between successive TLS scans, we compared point clouds along a shortest distance vector between a meshed reference scan and subsequent point clouds using the IMInspect module of Polyworks. Positive differences indicate gain of material or slope deformation and a negative difference indicates loss of material, such as a rockfall.

To detect small slope deformations, smaller than the limit of detection for a single point (0.022 to 0.036 m), we implemented a 3-Dimensional (3D) noise filtering algorithm on the TLS data, an extension to the 2D filtering method (Abellán et al., 2009). First we constructed a kd tree data structure for the reference and subsequent point clouds. We then calculated local surface normals for each point in the reference cloud using the best fit of a plane to the neighbouring 100 points. Thirdly, we calculated point cloud differences

from reference to successive scans at each point along these normal vectors by taking the mean of the dot product of the five closest Euclidean reference to data vectors with the normal vector. Lastly, for each point we calculated the median difference of 25 neighbours, reducing our per point limit of detection to 5-10 mm for this slope. We monitored identified areas of slope deformation over time by also calculating and analysing the statistical distributions of the area defined by the area of deformation.

These differences were then interpreted to represent accumulations of soil or rocky debris and discrete block deformation. For example, accumulation of debris at the base of the slope is easily recognized given the conical shape and characteristic surface roughness, while deformation of rock outcrop areas appears as displacement of discrete rock blocks. Systematic errors as a result of low incidence angle, poor surface reflectance and vegetation are typically distinguished by their implausible kinematics, or systematic expression.

We obtained the vector deformation magnitude and direction using three dimensional block tracking (Oppikofer et al., 2009; Teza et al., 2007). We used the ICP algorithm to fit the reference point cloud representation of the deforming block to each successive representation of the block in the successive point clouds followed by the extraction of the deformation magnitude and directions from the affine transformation matrices. Mean error in the magnitude was obtained by performing the method on 10 stable areas for various collection dates and was 0.008 m in each of the x, y and z directions. This analysis was only performed on the largest area of deformation.

We collected 162 oblique aerial photographs of the post-failure slope on 14 December 2014, using a Nikon D800 camera equipped with a 50 mm (f/1.8G) Nikon lens, during a helicopter overview flight. From these photos we built a 3D point cloud and meshed surface model using the 'structure from motion' approach of the commercial software package Photoscan (V1.021) by Agisoft (Agisoft, 2014).

Pre-failure volume was estimated based on the surface representation of the deformation and the defining discontinuities. The post-failure volumes were

calculated by comparing meshed pre-failure TLS model with the post-failure OHP model. Structural analysis was performed by manually identifying all of the points in point cloud on the discontinuity surface and best fitting a plane through them.

3 RESULTS

We identified three areas of slope deformation between scan dates December 2013 and June 2014 (noted as a., b. and c. in Figure 2). Differences at a. were greater than the single point limit of detection and the deformation could easily be interpreted from direct comparison of unfiltered data. Area a. consisted of a group of blocks, constrained by joints measured from the point cloud ($025^{\circ}/43^{\circ}$, $055^{\circ}/85^{\circ}$, $013^{\circ}/74^{\circ}$, $135^{\circ}/70^{\circ}$). We also identified differences directly upslope of area a.; this is interpreted to be the movement of soil associated with deformation of the rock. Area b. consists of a group of three blocks with a slope face orientation of ($133^{\circ}/73^{\circ}$). Area c. consists of two separate blocks. The top block had a well-defined back fracture (based on area of movement) with orientation of ($207^{\circ}/82^{\circ}$) and was bounded by joints ($245^{\circ}/84^{\circ}$, $180^{\circ}/63^{\circ}$, $331^{\circ}/78^{\circ}$). Based on the area of interpreted deformation and the bounding joint sets, we calculated a projected volume of failure of 4800 m^3 of rock and soil at a. as outlined in Figure 3. Volumes of blocks at b. and c. were not projected prior to failure due to their relatively small extent and perceived low risk.

Each of the three identified areas continued to deform (insets, Figure 2) after we gave early warning in September of 2014. The mean difference (reference date 28 November 2013) of the group of blocks at a. was calculated to be 0.045 m as of 4 June 2014, and increased to 0.049 m on 10 November 2014, prior to failure. The mean difference for the group of blocks at b. and c. ranged from 0.031 to 0.044 m and 0.010 to 0.021 m, respectively.

Using 3D block tracking from the reference scan representation of the deforming area at a. to 10 November 2014, we obtained a vector deformation magnitude of 0.10 m with a mean plunge of 14° towards 197° . We performed this analysis on the group of blocks at a. only, since the movement of blocks at b. and c. were within the error of this analysis method.

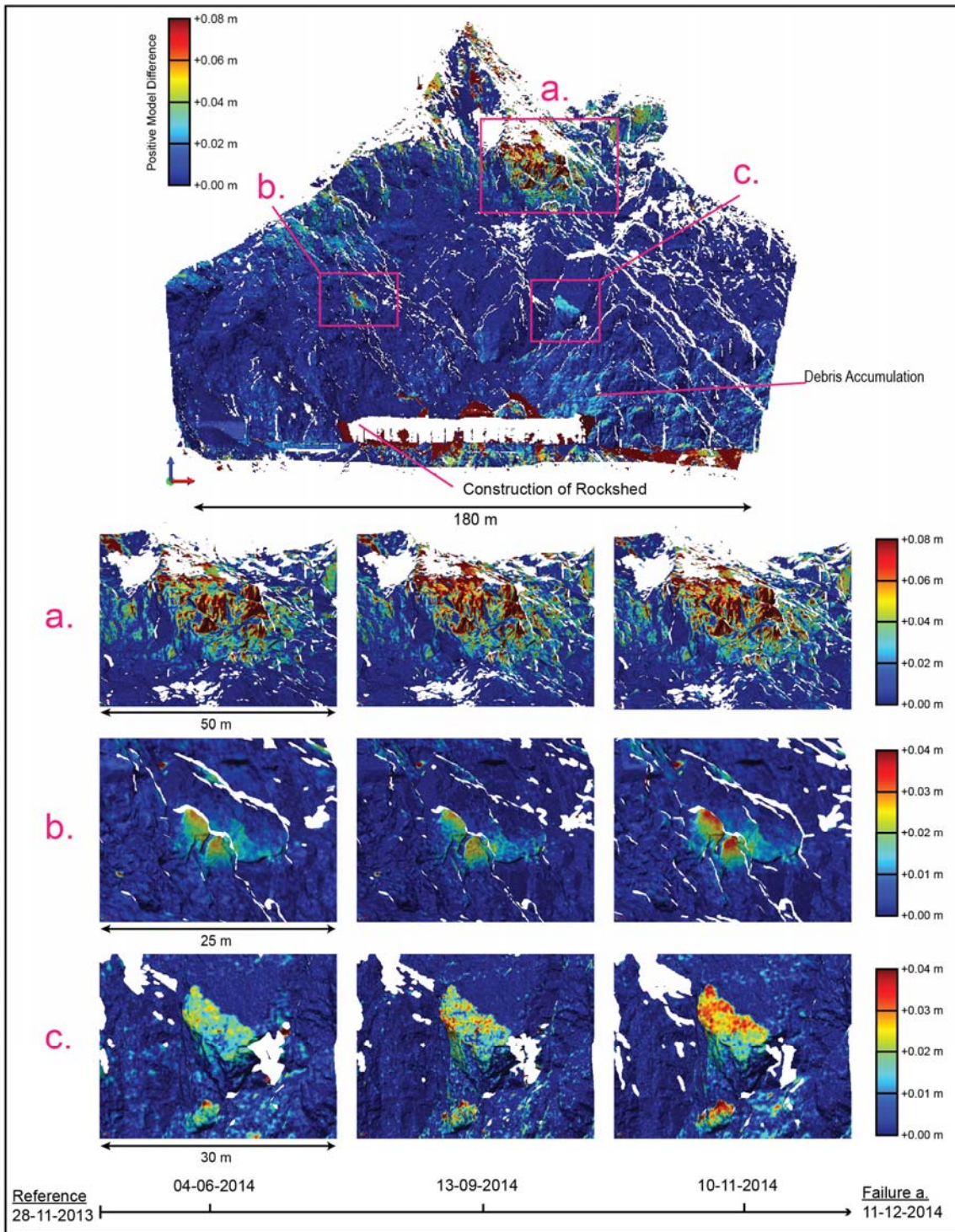
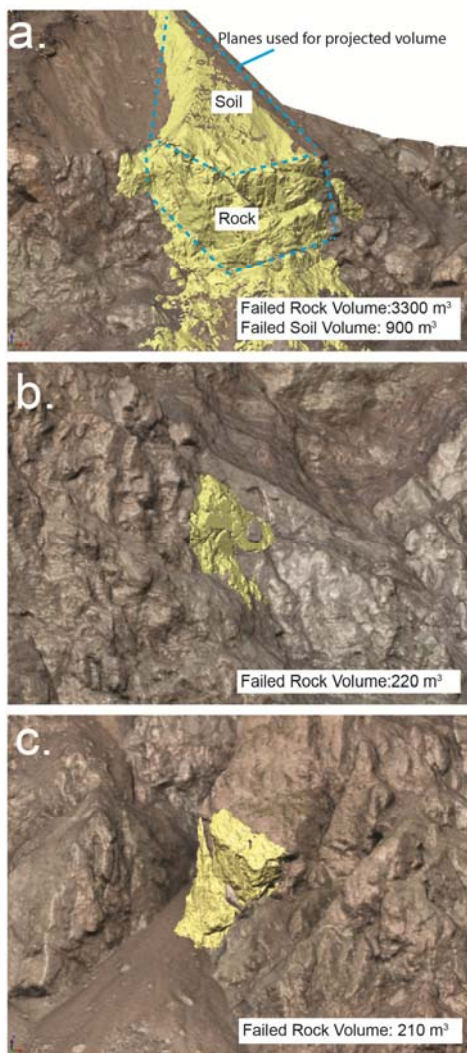


Figure 2: Three-dimensional analysis of slope deformation and deformation time series. Top: Filtered deformation image for the whole slope comparing reference scan 28-11-2013 with 10-11-2014 indicating deforming rock blocks identified prior to the failure. Bottom: Time series of identified areas of change prior to rockfall failure. Other observed slope change due to construction of rockfall protection structure (bottom) and accumulation of rock debris and soil.

Post failure, we detected three rockfall source zone areas using a comparison of Oblique Helicopter Photogrammetry (OHP) model and pre-failure TLS models, each directly corresponding to the previously identified areas of deformation (Figure 3). We calculated a depletion area volume at a. of 4200 m³, consisting of 3300 m³ of rock blocks and 900 m³ of overlaying soil. Failed volumes for areas b. and c. were 220 m³ and 210 m³, respectively. The post-failure planes at a. are consistent with those identified prior to failure, and lead to wedge-type kinematics, formed from the intersection of joints 025° /43° and 013° /74°, with sliding direction oriented approximately 188° /14°. This is consistent with results from the block tracking analysis prior to failure (197° /14°).



TLS 10-11-2014 (yellow) Photogrammetry 15-12-2014 (textured)

Figure 3: Analysis of post-rockfall failure volumes using OHP data. TLS model of source zones prior to failure overlain on after failure photogrammetry model and failed volumes for areas a., b., and c. Areas of failure correspond to predicted source zones outlined in Figure 2.

4 DISCUSSION

We interpret the observed accumulation of rock debris occurring prior to 3 December 2014 as rockfall precursors to the blocks at a., as no other source zone was identified in the difference between the OHP data and the TLS. We detected, through direct comparison TLS point clouds that hundreds of fragmental rockfalls smaller than 1 m³ had occurred throughout the year preceding these larger failures. We were unable to detect pre-failure deformation for these small volume rockfalls, possibly because the duration of precursor deformation was too rapid compared to the monitoring frequency and/or the pre-failure deformation was too small in magnitude and/or the rockmass did not behave in a progressive manner.

Rockfall activity in the region is affected by seasonal climatic effects including freeze-thaw cycles and precipitation (Peckover and Kerr, 1977). Beginning on 8 December 2014, three days prior to failure of area a., the region experienced 41 mm of rainfall, which we hypothesize to be the primary triggering factor for the failure events. Although we can only constrain the time of failure of blocks at b. and c. to be between 3 December and 11 December, we interpret a failure date during or shortly after this rainfall event. From analysis of post failure photographs, The debris accumulation from the rockfall source area a. appears to cover the debris accumulation below source zone b., indicating that rockfalls from source zone b. preceded a. We interpret rockfalls at this site (and others nearby) to be strongly dominated by environmental triggers such as rainfall and frost jacking with slope creep (progressive sliding or crack growth) occurring continuously, resulting in the observed deformation throughout the year (Crosta and Agliardi, 2003; Peckover and Kerr, 1977).

Our monitoring frequency was sufficient to capture the pre-failure deformation for the December 2014 events, however it was not frequent enough to capture an accelerating phase prior to failure, which is necessary for temporal forecasting (Crosta and Agliardi, 2003). We also did not detect precursors rockfalls using our TLS comparisons, which could also be due to insufficient sampling prior to failure of the three blocks. Observations of small magnitude rockfall events made by railway employees prior to the failure and that only three source areas were identified post failure suggests that precursor rockfalls had occurred.

Most importantly, our prediction of potential source location, volume and kinematics was consistent with observations post failure. This ability to detect, locate and quantify hazard source zones with accurate volume estimation and kinematics prior to failure will result in an improved ability to prioritize mitigation efforts, reduce risk, and better understand slope failure mechanisms. This will ultimately improve safety of people and property exposed to many types of slope hazards, particularly rockfall and related landslide types. Future work should include higher frequency monitoring prior to failure for the forecasting of failure time.

5 CONCLUSIONS

In this study we have identified three areas of discrete rock block deformation on a complex slope traversed by an active rail line, projected the potential failure volume, tracked the deformation in 3D and provided early warning to the railway prior to failure for the largest of the three. Our predictions of failure location, potential volume and kinematics were consistent with analysis results post failure. This monitoring approach can be used to provide advance warning of slope hazards in areas of vulnerability, and will ultimately result in reduced risk to communities and infrastructure. This is especially important as our growing population expands into more hazardous areas.

ACKNOWLEDGEMENTS

We would like to acknowledge support from our funding agencies: CN Rail, CP Rail, Transport Canada and the National Sciences and Engineering Research Council of Canada (NSERC). Special thanks to Matthew Ondercin and Megan van Veen from Queen's University for aid in field data collection; Trevor Evans from CN Rail for organizing helicopter data collection; Chris Bunce from CP Rail for allowing site access; and Brad Forbes, Chrysothemis Paraskevopoulou, and Rob Harrap from Queen's and Wayne Savigny from BGC Engineering for suggestions regarding the written work.

REFERENCES

- Abellán, A., Calvet J., Vilaplana, J.M. and Blanchard J. 2010. Detection and spatial prediction of rockfalls by means of terrestrial laser scanner monitoring. *Geomorphology*, 119: 162–171.
- Abellán, A., Jaboyedoff, M., Oppikofer, T. and Vilaplana J.M. 2009. Detection of millimetric deformation using a terrestrial laser scanner: experiment and application to a rockfall event. *Natural Hazards and Earth System Science*, 9: 365–372.
- Agisoft. Photoscan. 2014. v1.0. St. Petersburg, Russia.
- Crosta, G.B. and Agliardi, F. 2003. Failure forecast for large rock slides by surface displacement measurements. *Canadian Geotechnical Journal*, 40: 176–191.
- Eberhardt, E., Stead, D. and Coggan, J.S. 2004. Numerical analysis of initiation and progressive failure in natural rock slopes—the 1991 Randa rockslide. *International Journal of Rock Mechanics and Mining Sciences* 41: 69–87.
- Environment Canada. 2014. Daily Climate Data (Hope). <http://climate.weather.gc.ca>.
- InnovMetric. 2014. PolyWorks V14. Quebec City, Canada.
- Lato, M.J., Diederichs, M.S., Hutchinson D.J. and Harrap R. 2011. Evaluating roadside rockmasses for rockfall hazards using LiDAR data: optimizing data collection and processing protocols. *Natural Hazards and Earth System Science*, 60: 831–864.
- Lato M.J., Hutchinson D.J., Gauthier D., Edwards T. and Ondercin M. 2014. Comparison of ALS, TLS and terrestrial photogrammetry for mapping differential slope change in mountainous terrain. *Canadian Geotechnical Journal*.
- Lim, M., Petley, D.N., Rosser, N.J., Allison, R.J., Long, A.J. and Pybus D. 2005. Combined Digital Photogrammetry and Time-of-Flight Laser Scanning for Monitoring Cliff Evolution. *The Photogrammetric Record*, 20: 109–129.
- Oppikofer, T., Jaboyedoff, M., Blikra, L., Derron, M.H. and Metzger, R. 2009. Characterization and monitoring of the Åknes rockslide using terrestrial laser scanning. *Natural Hazards and Earth System Science*, 9 : 1003–1019.
- Oppikofer, T., Jaboyedoff, M., Keusen, H-R. 2008. Collapse at the eastern Eiger flank in the Swiss Alps. *Nature Geoscience*, 1: 531–535.
- Optech. 2014. ILRIS-3D Intelligent Laser Ranging and Imaging Systems. <http://www.optech.com>.
- Peckover, F.L. and Kerr J.W.G. 1977. Treatment and maintenance of rock slopes on transportation routes. *Canadian Geotechnical Journal*, 14: 487–507.
- Petley, D.N. 2004. The evolution of slope failures: mechanisms of rupture propagation. *Natural Hazards and Earth System Science*, 4: 147–152.
- Rosser, N., Lim, M., Petley, D., Dunning, S. and Allison, R. 2007. Patterns of precursory rockfall prior to slope failure. *Journal of Geophysical Research*, 112.
- Rosser, N.J., Petley, D.N., Lim, M., Dunning, S.A. and Allison, R.J. 2005. Terrestrial laser scanning for monitoring the process of hard rock coastal cliff erosion. *Quarterly Journal of Engineering Geology and Hydrogeology*, 38: 363–375.
- Royán, M.J., Abellán, A., Jaboyedoff, M., Vilaplana, J.M. and Calvet J. 2013. Spatio-temporal analysis of rockfall pre-failure deformation using Terrestrial LiDAR. *Landslides*, 11: 697–709.
- Stock, G.M., Martel, S.J., Collins, B.D. and Harp, E.L. 2012. Progressive failure of sheeted rock slopes: the 2009-2010 Rhombus Wall rock falls in Yosemite Valley, California, USA. *Earth Surface Processes and Landforms*, 37: 546–561.
- Sturzenegger, M., Keegan, T., Wen, A., Willms, D. Stead, D. and Edwards T. 2014. LiDAR and Discrete Fracture Network Modeling for Rockslide Characterization and Analysis. *In Engineering Geology for Society and Territory - Volume 6*, Lollino G, Giordan D, Thuro K, Carranza-Torres C, Wu F, Marinos P, and Delgado C (eds). Springer International Publishing, 223–227.
- Sturzenegger, M. and Stead, D. 2009. Close-range terrestrial digital photogrammetry and terrestrial laser scanning for discontinuity characterization on rock cuts. *Engineering Geology*, 106: 163–182.
- Teza, G., Galgaro, A., Zaltron, N. and Genevois, R. 2007. Terrestrial laser scanner to detect landslide displacement fields: a new approach. *International Journal of Remote Sensing*, 28: 3425–3446.